Arch. Mech., 38, 5–6, pp. 611–634, Warszawa 1986

A computational model for the prediction of two-dimensional non-equilibrium turbulent recirculating two-phase flow(*)

B. DOBROWOLSKI (OPOLE)

A COMPUTATIONAL model for the prediction of elliptical, non-equilibrium turbulent two-phase flow of a dilute mixture has been formulated. The model is based on a two-velocity field method for the description of the hydrodynamic non-equilibrium flow. A new form of the motion and turbulence model equations has been obtained by time-averaging of the motion equations for laminar flow and by neglecting the turbulent correlations of volume fraction fluctuations. A series of calculations for two-dimensional recirculating flow based on the proposed computational algorithm has been presented. A considerable influence of particle diameters of the dispersed phase and the non-equilibrity of flow on the local and global characteristics of two-phase stream has been found. A simple form of the correction function, based on four non-dimensional similarity groups, has been proposed for the calculation of the pressure drop in case of transitionally non-equilibrium dispersed two-phase flow.

Sformułowano model matematyczny do obliczania eliptycznych, nierównowagowych przepływów turbulentnych rozrzedzonych mieszanin dwufazowych. Model oparto na metodzie dwupolowej dla uwzględnienia hydrodynamicznej nierównowagowości zjawiska przepływu. Nową postać równania ruchu i modelu turbulencji otrzymano przez uśrednienie równań dla przepływu laminarnego, przy pominięciu korelacji fluktuacji udziału objętościowego faz. Przedstawiono modyfikację $k-\varepsilon$ modelu turbulencji w celu uwzględnienia turbulentnych oddziaływań międzyfazowych. Opracowano algorytmy obliczeń oraz zrealizowano serię obliczeń dla dwuwymiarowego przepływu z recyrkulacją. Stwierdzono duży wpływ średnicy cząstek fazy rozproszonej oraz przejściowej nierównowagowości przepływu na lokalne i globalne charakterystyki strugi dwufazowej. Zaproponowano prostą funkcję korekcyjną opartą na czterech bezwymiarowych liczbach podobieństwa do obliczania straty ciśnienia przy przejściowo-nierównowagowym dyspersyjnym przepływie dwufazowym.

Сформулирована математическая модель для расчета эллиптических, неравновесных турбулентных течений разреженных двухфазных смесей. Модель опирается на двуполевый метод для учета гидродинамического неравновесия явления течения. Новый вид уравнения движения и модели турбулентности получен путем усреднения уравнений для ламинарного течения, при пренебрежении корреляциями флуктуации объемного участия фаз. Представлена модификация $k-\varepsilon$ модели турбулентности с целью учета турбулентных межфазных взаимодействий. Разработаны алгоритмы расчетов для двумерного течения с рециркуляцией. Констатировано большое влияние диаметра частиц рассеянной фазы и переходного неравновесия течения на локальные и глобальные характеристики двухфазной струи. Предложена простая коррекционная функция, опирающаяся на четырех безразмерных числах подобия, для расчета потери давления при переходно-неравновесном дисперсионном двухфазном течении.

1. Introduction

THE HOMOGENEOUS model used traditionally for two-phase flow calculations is based on the assumption of thermal and mechanical equilibrium between phases and it is not capable

(*) Paper given at XVII Symposium on Advanced Problems and Methods in Fluid Mechanics, Sobieszewo, 2–6 September 1985.

of predicting the flow distribution under conditions which cause departure from the equilibrium. In the case of a thermal or mechanical non-equilibrium flow, a more complex approach is needed for the prediction of the local and global flow characteristics.

There are basically two methods for the calculation of two- or multi-phase non-equilibrium flow: the multi-fluid method and the trajectory method. The average equations which describe the continuous and dispersed phases as two interactive fluids are the basis of the two-fluid method. Some examples of computational schemes, based on the two-fluid approach, are given by HARLOW and AMSDEN [1], RIVARD and TORREY [2], and SPALDING [3]. Although the two-fluid models, applied to diluted dispersed flow, have the advantage of using numerical procedures already established for single-phase flow, there are some difficulties in their use. When treating more than one particle size, it is necessary to regard each size category as a separate fluid which demands considerably more computer time and storage than in the case of a single phase flow.

The other possibility of modelling dispersed two- or multi-phase flows is the trajectory approach, first proposed by MIGDAL and AGOSTA [4] and then developed by CROWE *et al.* [5] and DUKOWICZ [6]. This method, called the PSI-Cell model, is based on the idea of introducing the Lagrangian approach for the motion of the dispersed phase. The model incorporates the most natural computational scheme for each phase, namely the relaxation method for the continuos phase and the marching method for the disperse phase. The PSI-Cell approach, however, seems to be not quite suitable for the two-way coupling solutions and requires in any case an additional computation effort to evaluate the source terms introduced by particles in the continuous phase equations.

In the case of turbulent flow it is necessary to introduce the turbulent interphase interactions into the models. As shown in some new measurements performed by MAEDA and HISHIDA [7], TSUJI *et al.* [8] and MODARRES *et al.* [9], the presence of particles or droplets exerts an influence both on the time-mean characteristics of turbulent two-phase stream and the turbulence structure.

In the DUKOWICZ [6] model, the particle dispersion, due to turbulence, is modelled by the diffusion force requiring the selection of a diffusion coefficient. The other technique is based on the Monte Carlo method, presented by GOSMAN and IOANNIDES [10], in which the turbulent gas flow field is modelled as a steady flow plus random velocity fluctuations. DANON *et al.* [11] attempted to develop a one-equation turbulence model based on the modified equation of the turbulence kinetic energy and an empirically prescribed length scale. The differences between the results of calculations and experimental data were large so that some arbitrary empirical corrections were introduced into the model in order to achieve agreement with the data.

Recently, ELGHOBASHI *et al.* [12, 13, 14] have presented a new computational model for two-dimensional, parabolic, turbulent dispersed two-phase flow. In the paper [12] some new forms of the motion and turbulence model equations were proposed, by modelling all new correlations to the third order inclusive. Some new additional terms and constants were introduced into the standard form of the LAUNDER and SPALDING [15] $k-\varepsilon$ turbulence model. The proposed calculation method was applied in the computation of gas-particle [13] and gas-droplet [14] free stream flow and good agreement with the experimental data was achieved.

The disadvantage of the ELGOBASHI and ABOU-ARAB [12] model is its considerable complexity even in the case of a parabolic flow. Moreover, there is no information whether the additional empirical constants are of universal character or if the model may be used in an elliptical flow with a large pressure gradient and with the presence of walls.

The aim of the present paper is to formulate a simplified physical and computational model for the prediction of recirculating, two-phase flow of a dilute suspension of dense particles in air. The computational model is then applied in the prediction of the effects of the interaction phenomena and transitional non-equilibrium between the two-phases in the two-dimensional, recirculating flow system.

2. General formulation of mathematical model equations

2.1. Two-phase motion equations in the case of laminar flow

It is assumed that a two-phase mixture is a dilute suspension and both phases are microscopically incompressible. Two-phase flow is treated as the motion of interpenetrating and interacting continuous fluids. The steady motion of both components is described by the set of equations

$$\nabla\cdot\alpha_d\mathbf{U}_d = 0, \tag{2.1}$$

$$\nabla\cdot\alpha_c\mathbf{U}_c = 0, \tag{2.2}$$

$$\varrho_d\nabla\cdot\alpha_d\mathbf{U}_d\mathbf{U}_d = -\alpha_d\nabla p + F(\mathbf{U}_c-\mathbf{U}_d)+\alpha_d\mathbf{g}\varrho_d, \tag{2.3}$$

$$\varrho_c\nabla\cdot\alpha_c\mathbf{U}_c\mathbf{U}_c = -\alpha_c\nabla p + F(\mathbf{U}_d-\mathbf{U}_c)+\nabla\cdot\alpha_c\mu_c(\nabla\mathbf{U}_c+\nabla\mathbf{U}_c^T)+\alpha_c\mathbf{g}\varrho_c, \tag{2.4}$$

where α denotes volume fraction, $\mathbf{U}$ is the velocity vector, p is pressure, ϱ is density, μ is viscosity and the subscripts c and d concern the continuous and dispersed phases, respectively.

The dispersed phase is treated as inviscid on account of the absence of any physical interpretation of the molecular viscosity of this phase in case of dilute suspensions. The set of equations (2.1)–(2.4) is commonly used for describing laminar flow of monodispersed mixtures [16]. Equation (2.4) points at the elliptic nature of motion of the continuous phase and Eq. (2.3) at the rather parabolic nature of motion of the dispersed phase. The modified interphase friction coefficient F is calculated from the formula

$$F = \alpha_d\frac{18\mu_c}{(d_p)^2}f_D \tag{2.5}$$

by assuming Stokes' flow around a particle, f_D is the empirical correction factor.

It is further assumed that the set of equations (2.1)–(2.4) describes correctly the laminar flow of a certain class of two-phase mixtures and the quantity f_D has a constant value locally.

2.2. Two-phase motion equations in the case of turbulent flow

The instantaneous values of dependent variables consist of mean and fluctuating components:

$$\mathbf{U}_c = \mathbf{U}_c+\mathbf{u}_c', \quad \mathbf{U}_d = \bar{\mathbf{U}}_d+\mathbf{u}_d', \quad p = \bar{p}+p', \quad \alpha = \bar{\alpha}+\alpha'.$$

Further considerations are limited to the situation when phase densities vary considerably ($\varrho_d/\varrho_c \sim 10^3$) and the volume fraction of the dispersed phase is low ($\alpha_d < 10^{-2}$). The apparent density of gas $\tilde{\varrho}_c = \alpha_c \varrho_c$ is then within the interval $0.99\ \varrho_c \leqslant \tilde{\varrho}_c \leqslant \varrho_c$; in this connection the gaseous phase can be treated as macroscopically incompressible and the volume fraction fluctuation may be ignored.

After performing the conventional Reynolds averaging and after approximating the Reynolds stress tensors, the mean flow equations for both phases can be written down in the form

$$\nabla \cdot \bar{\alpha}_d \bar{\mathbf{U}}_d = 0, \tag{2.6}$$

$$\nabla \cdot \bar{\alpha}_c \bar{\mathbf{U}}_c = 0, \tag{2.7}$$

$$\varrho_d \nabla \cdot \bar{\alpha}_d \bar{\mathbf{U}}_d \bar{\mathbf{U}}_d = -\bar{\alpha}_d \nabla \bar{p} + F(\bar{\mathbf{U}}_c - \bar{\mathbf{U}}_d) + \bar{\alpha}_d \mathbf{g} \varrho_d + \nabla \cdot \bar{\alpha}_d \mu_{dt} (\nabla \bar{\mathbf{U}}_d + \nabla \bar{\mathbf{U}}_d^T), \tag{2.8}$$

$$\varrho_c \nabla \cdot \bar{\alpha}_c \bar{\mathbf{U}}_c \bar{\mathbf{U}}_c = -\bar{\alpha}_c \nabla \bar{p} + F(\bar{\mathbf{U}}_d - \bar{\mathbf{U}}_c) + 2/3 \varrho_c \bar{\alpha}_c \nabla k + \alpha_c \mathbf{g} \varrho_c + \nabla \cdot \bar{\alpha}_c \mu_{ef} (\nabla \bar{\mathbf{U}}_c + \nabla \bar{\mathbf{U}}_c^T). \tag{2.9}$$

The turbulent stress tensor for the continuous phase is calculated on the basis of the Kolmogorov–Prandtl hypothesis

$$-\varrho_c \overline{\mathbf{u}_c' \mathbf{u}_c'} = \mu_t (\nabla \bar{\mathbf{U}}_c + \nabla \bar{\mathbf{U}}_c^T) - 2/3 \boldsymbol{\delta} \varrho_c k, \tag{2.10}$$

where $\mu_{ef} = \mu_c + \mu_t$ and the turbulent viscosity μ_t is calculated on the basis of the $k-\varepsilon$ turbulence model

$$\mu_t = c_\mu \varrho_c k^2/\varepsilon. \tag{2.11}$$

The quantities k and ε are computed by some additional transport equations obtained by the modification of the LAUNDER and SPALDING [15] turbulence model.

It is assumed that the turbulent stress tensor for the dispersed phase is dependent on the turbulent viscosity μ_{dt} on the particle field

$$-\varrho_d \overline{\mathbf{u}_d' \mathbf{u}_d'} = \mu_{dt} (\nabla \bar{\mathbf{U}}_d + \nabla \bar{\mathbf{U}}_d^T). \tag{2.12}$$

It can be noticed that the definition (2.12) is of an arbitrary character and it is assumed rather by analogy to Eq. (2.10) than on the basis of strict physical reasons. This results from the great difficulty to formulate constitutive equations for the dispersed systems as found by DOBRAN [17] and DREW and LAHEY [18].

According to the well-known PESKIN [19] formula, the quantity μ_{dt} for the particle field may be calculated by introducing the turbulent Schmidt number σ_p for the particles

$$\frac{\mu_{dt} \varrho_c}{\mu_t \varrho_d} = \frac{1}{\sigma_p} = 1 - \frac{3}{2} \left(\frac{L_L}{\lambda} \right)^2 \frac{Q^2}{Q+2}, \tag{2.13}$$

where

$$Q = 2\varrho_d / F T_L$$

as a function of particle properties and the turbulence structure. Assuming the isotropic turbulence, the local Lagrangian time scale T_L can be expressed by the equation

$$T_L = \frac{5}{12} k/\varepsilon. \tag{2.14}$$

The local Lagrangian length scale L_L and the Eulerian microscale λ are given by

$$L_L = \sqrt{\frac{2}{3}k}\,T_L, \tag{2.15}$$

$$\lambda = \sqrt{10\nu_c k/\varepsilon}. \tag{2.16}$$

As a result of time averaging and introducing the definition (2.12), the equation of motion for the dispersed phase (2.8) is elliptical which means that there occurs an exchange of momentum between particles resulting from turbulent particle collisions.

2.3. Equations of turbulence model

The presence of the interphase momentum exchange function F in the motion equation (2.4) results in the occurrence of new correlations in transport equations for the turbulence kinetic energy k and its dissipation rate ε. The strict correlational form of transport equations for k and ε are given by ELGHOBASHI and ABOU-ARAB [12]. In the case of two-phase flow the exact equation for the turbulence kinetic energy consists of 38 terms and for the dissipation rate, of 67 terms.

On some additional assumptions, mentioned in Sect. 2.2, and after modelling the well-known turbulent correlations, the transport equation for k has the form

$$\varrho_c \nabla\cdot\bar{\alpha}_c k\bar{\mathbf{U}}_c = \nabla\cdot\bar{\alpha}_c \frac{\mu_t}{\sigma_k}\nabla k + \bar{\alpha}_c(\mu_t G - \varrho_c \varepsilon) + S_p^k, \tag{2.17}$$

where S_p^k denotes the additional source term. This term has the form

$$S_p^k = F(\overline{u'_{ci}u'_{di}} - 2k) \tag{2.18}$$

and only one new correlation has to be approximated. A similar form of the term S_p^k was obtained by DANON *et al.* [11] and GENCHEV and KARPUZOV [20].

With the assumption $\overline{u'_{ci}u'_{di}} = 2k$ in the case of very small particles, the term $S_p^k = 0$ and then the two-phase mixture can be considered as the homogeneous mixture. When particles are not subject to gas velocity fluctuations, that is $\overline{u'_{ci}u'_{di}} = 0$, then $S_p^k = -2Fk$ and the dispersed phase significantly reduces the kinetic energy of turbulence of the continuous phase. On the basis of the CHAO [21] solution of the motion equation of a spherical particle in a turbulent fluid, as shown by ELGHOBASHI and ABOU-ARAB [12], it is possible to evaluate the value of the correlation $\overline{u'_{ci}u'_{di}}$ and the term S_p^k may be written down in the form

$$S_p^k = -\bar{\alpha}_c \varrho_c \varepsilon_a = -\bar{\alpha}_c \varrho_c \left[\frac{Fk}{\bar{\alpha}_c \varrho_c}\left(1 - \int_0^\infty \frac{\Omega_1 - \Omega_R}{\Omega_2} E(\omega)\,d\omega\right)\right], \tag{2.19}$$

where $E(\omega)$ is the Lagrangian frequency function. The function $E(\omega)$ is, in general, affected by the presence of particles. In the low frequency range (inertial subrange) the modulation of the Lagrangian frequency function of the continuous phase by the dispersed phase can be neglected as shown by TSUJI *et al.* [8]. Thus the following form of the function $E(\omega)$ can be used:

$$E(\omega) = \frac{2}{\pi} \frac{T_L}{1+\omega^2 T_L^2}, \tag{2.20}$$

where ω ranges from 1 to 10^4 and T_L is calculated from Eq. (2.14)

The functions Ω_1, Ω_2 and Ω_R are evaluated on the basis of the CHAO [21] solutions

$$\Omega_1 = \left(\frac{\omega}{\alpha}\right)^2 + \sqrt{6}\left(\frac{\omega}{\alpha}\right)^{3/2} + 3\left(\frac{\omega}{\alpha}\right) + \sqrt{6}\left(\frac{\omega}{\alpha}\right)^{1/2} + 1,$$

$$\Omega_2 = \beta^{-2}\left(\frac{\omega}{\alpha}\right)^2 + \sqrt{6}\beta^{-1}\left(\frac{\omega}{\alpha}\right)^{3/2} + 3\left(\frac{\omega}{\alpha}\right) + \sqrt{6}\left(\frac{\omega}{\alpha}\right)^{1/2} + 1,$$

$$\Omega_R = [(1-\beta)\omega/(\alpha\beta)]^2,$$

where

$$\alpha = 12\nu_c f_D/d_p^2, \qquad \beta = 3\varrho_c/(2\varrho_d+\varrho_c).$$

The quantity ε_a in Eq. (2.19) represents the additional dissipation of the turbulence kinetic energy connected with turbulent interphase interactions. Since the value of the integral in Eq. (2.19) is within the interval $\langle -1, +1\rangle$, the value of the term S_p^k is limited to the interval

$$0 \geqslant S_p^k \geqslant -2Fk. \tag{2.21}$$

The transport equation for the dissipation rate ε, developed on the basis of Eq. (2.2), has the form

$$\varrho_c \nabla\cdot\bar{\alpha}_c \varepsilon \bar{U}_c = \nabla\cdot\bar{\alpha}_c \frac{\mu_t}{\sigma_\varepsilon} \nabla\varepsilon + \bar{\alpha}_c \frac{\varepsilon}{k}(c_1\mu_t G - c_2\varrho_c\varepsilon) + S_p^\varepsilon, \tag{2.22}$$

where S_p^ε is related to the presence of the function F in the motion equations. The strict form of the S_p^ε term for the considered class of the two-phase flow is given by the equation

$$S_p^\varepsilon = 2F\left(\nu_c \overline{\frac{\partial u'_{ci}}{\partial x_k}\frac{\partial u'_{di}}{\partial x_k}} - \varepsilon\right) + \nu_c \frac{\partial F}{\partial x_k}\left(\overline{2u'_{di}\frac{\partial u'_{ci}}{\partial x_k}} - \frac{\partial k}{\partial x_k}\right). \tag{2.23}$$

The value of S_p^ε is within the interval

$$0 \geqslant S_p^\varepsilon \geqslant -2F\varepsilon - \nu_c \nabla F\cdot\nabla k. \tag{2.24}$$

Considering that $F \gg \nu_c$, the second term in Eq. (2.24) may be neglected and the value of S_p^ε can be evaluated in the following way

$$S_p^\varepsilon = 2F\left(\nu_c \overline{\frac{\partial u'_{ci}}{\partial x_k}\frac{\partial u'_{di}}{\partial x_k}} - \varepsilon\right) = -\frac{\varepsilon}{k}\alpha_c\varrho_c\varepsilon_a, \tag{2.25}$$

where ε_a is determined by Eq. (2.19). The value of S_p^ε is within the interval $0 \geqslant S_p^\varepsilon \geqslant -2F\varepsilon$. Thus the maximum value of the term is different from the maximum value of the expression (2.23) only about a negligible low value of the expression $\nu_c \nabla F\cdot\nabla k$.

As a result of some additional assumptions, the proposed forms of the equations of motion and those of the turbulence model are considerably simpler than the ones given by ELGHOBASHI and ABOU-ARAB [12]. Some new components have been introduced in a strict manner with no need to introduce any additional empirical constants. The evaluation carried out indicate that the quantities S_p^ε and S_p^k display correct asymptotical behaviour with the change of a particle diameter.

3. Application of the model to two-dimensional recirculating flow

3.1. The flow considered and equations

The presented mathematical model is applied in the calculation of a two-phase flow through a pipe orifice. In the considered geometrical configuration, shown in Fig. 1, which may schematically represent the flow metering system, the sudden throat restriction gener-

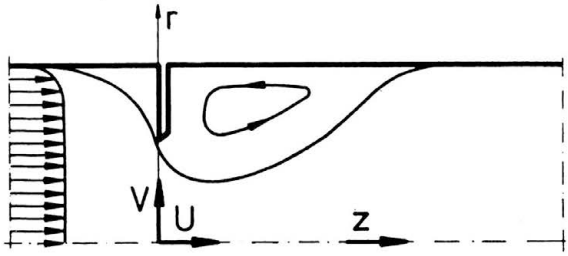

FIG. 1. Flow system with an orifice-meter.

ates substantial accelerations and transitional non-equilibrium between the two phases. Since the recirculation zone exists behind the orifice, the flow phenomenon is of an elliptical character. The axial symmetry is assumed, the gravitational force is neglected, and Eqs. (2.6)–(2.9), (2.17) and (2.22) are simplified to two-dimensional ones and they are written down in the cylindrical coordinates. With the above assumptions the motion of the two-phase mixture is described by a set of equations, which consists of the following equations of continuity

$$\frac{\partial}{\partial z}(\alpha_d U_d)+\frac{1}{r}\frac{\partial}{\partial r}(r\alpha_d V_d)=0, \tag{3.1}$$

$$\frac{\partial}{\partial z}(\alpha_c U_c)+\frac{1}{r}\frac{\partial}{\partial r}(r\alpha_c V_c)=0, \tag{3.2}$$

equations of motion for the continuous phase

$$\varrho_c\left\{\frac{\partial}{\partial z}(\alpha_c U_c^2)+\frac{1}{r}\frac{\partial}{\partial r}(r\alpha_c U_c V_c)\right\}=-\alpha_c\frac{\partial p}{\partial z}+\frac{2}{3}\alpha_c\varrho_c\frac{\partial k}{\partial z}+F(U_d-U_c)+2\frac{\partial}{\partial z}\left(\alpha_c\mu_{ef}\frac{\partial U_c}{\partial z}\right)+\frac{1}{r}\frac{\partial}{\partial r}\left(r\alpha_c\mu_{ef}\frac{\partial U_c}{\partial r}\right)+\frac{1}{r}\frac{\partial}{\partial r}\left(r\alpha_c\mu_{ef}\frac{\partial V_c}{\partial z}\right), \tag{3.3}$$

$$\varrho_c\left\{\frac{\partial}{\partial z}(\alpha_c U_c V_c)+\frac{1}{r}\frac{\partial}{\partial r}(r\alpha_c V_c^2)\right\}=-\alpha_c\frac{\partial p}{\partial r}+\frac{2}{3}\alpha_c\varrho_c\frac{\partial k}{\partial r}+F(V_d-V_c)+\frac{2}{r}\frac{\partial}{\partial r}\left(r\alpha_c\mu_{ef}\frac{\partial V_c}{\partial r}\right)+\frac{\partial}{\partial z}\left(\alpha_c\mu_{ef}\frac{\partial V_c}{\partial z}\right)+\frac{\partial}{\partial z}\left(\alpha_c\mu_{ef}\frac{\partial U_c}{\partial r}\right)-2\alpha_c\mu_{ef}\frac{V_c}{r^2} \tag{3.4}$$

and equations of motion for the dispersed phase:

$$(3.5)\quad \varrho_d\left\{\frac{\partial}{\partial z}(\alpha_d U_d^2)+\frac{1}{r}\frac{\partial}{\partial r}(r\alpha_d U_d V_d)\right\} = -\alpha_d\frac{\partial p}{\partial z} + F(U_c-U_d)+2\frac{\partial}{\partial z}\left(\alpha_d\mu_{dt}\frac{\partial U_d}{\partial z}\right)+\frac{1}{r}\frac{\partial}{\partial r}\left(r\alpha_d\mu_{dt}\frac{\partial U_d}{\partial r}\right) + \frac{1}{r}\frac{\partial}{\partial r}\left(r\alpha_d\mu_{dt}\frac{\partial V_d}{\partial z}\right),$$

$$(3.6)\quad \varrho_d\left\{\frac{\partial}{\partial z}(\alpha_d U_d V_d)+\frac{1}{r}\frac{\partial}{\partial r}(r\alpha_d V_d^2)\right\} = -\alpha_d\frac{\partial p}{\partial r} + F(V_c-V_d)+\frac{2}{r}\frac{\partial}{\partial r}\left(r\alpha_d\mu_{dt}\frac{\partial V_d}{\partial r}\right)+\frac{\partial}{\partial z}\left(\alpha_d\mu_{dt}\frac{\partial V_d}{\partial z}\right) + \frac{\partial}{\partial z}\left(\alpha_d\mu_{dt}\frac{\partial U_d}{\partial r}\right)-2\alpha_d\mu_{dt}\frac{V_d}{r^2},$$

where U and V are the mean velocities in the axial z and radial r directions, respectively. The interphase momentum exchange function F is calculated from Eq. (2.5) where the empirical correction factor f_D is given by

$$(3.7)\quad f_D = 1+0.15\,\mathrm{Re}_p^{0.687}$$

and Re_p denotes the particle Reynolds number based on the local interphase slip

$$(3.8)\quad \mathrm{Re}_p = \frac{\sqrt{(U_c-U_d)^2+(V_c-V_d)^2}\,\varrho_c d_p}{\mu_c}.$$

The turbulent viscosity of the dispersed phase μ_{dt} is calculated from Eq. (2.13). It has been found, however, that the Peskin formula in the present calculations gives a negative Schmidt number in most of the flow domain. A similar conclusion was reached in [13] for a two-phase turbulent jet expansion problem where the scale ratio L_L/λ in Eq. (2.13) was replaced by l/R where R is a stream radius and l is the dissipation length scale calculated from

$$(3.9)\quad l = C_\mu^{3/4}k^{3/2}/\varepsilon.$$

Due to the absence of any better information, Eq. (3.9) was applied in a part of the presented computations.

The turbulence model consists of the transport equations for the turbulence kinetic energy:

$$(3.10)\quad \varrho_c\left\{\frac{\partial}{\partial z}(\alpha_c U_c k)+\frac{1}{r}\frac{\partial}{\partial r}(r\alpha_c V_c k)\right\} = \frac{\partial}{\partial z}\left(\alpha_c\frac{\mu_t}{\sigma_k}\frac{\partial k}{\partial z}\right) + \frac{1}{r}\frac{\partial}{\partial r}\left(r\alpha_c\frac{\mu_t}{\sigma_k}\frac{\partial k}{\partial r}\right)+\alpha_c\mu_t G-\alpha_c\varrho_c\varepsilon+S_p^k,$$

and the dissipation ratio

$$(3.11)\quad \varrho_c\left\{\frac{\partial}{\partial z}(\alpha_c U_c \varepsilon)+\frac{1}{r}\frac{\partial}{\partial r}(r\alpha_c V_c \varepsilon)\right\} = \frac{\partial}{\partial z}\left(\alpha_c\frac{\mu_t}{\sigma_\varepsilon}\frac{\partial \varepsilon}{\partial z}\right) + \frac{1}{r}\frac{\partial}{\partial r}\left(r\alpha_c\frac{\mu_t}{\sigma_\zeta}\frac{\partial \varepsilon}{\partial r}\right)+\alpha_c\frac{\varepsilon}{k}(c_1\mu_t G-c_2\varrho_c\varepsilon)+S_p^\varepsilon,$$

where the terms S_p^k and S_p^ε are calculated from Eqs. (2.19) and (2.25).

The standard values of the $k-\varepsilon$ turbulence model constants were applied as given by LAUNDER and SPALDING [15] and RODI [22].

As a result, the set of eight nonlinear partial differential equations with eight unknowns U_c, V_c, U_d, V_d, p, k, ε and α_d is obtained. The volume fraction α_c of the continuous phase can be calculated from the global balance equation

$$\alpha_c + \alpha_d = 1,$$

3.2. Boundary conditions

The computational area, considered in further calculations, is presented in Fig. 2.

On account of the elliptical type of partial differential equations given in Sect. 3.1, it is necessary to assume appropriate boundary conditions for all the dependent variables on the area boundaries.

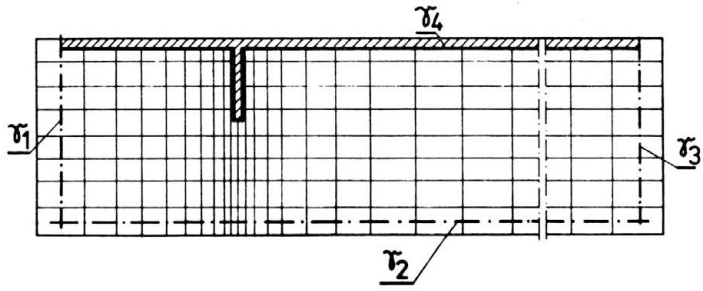

FIG. 2. The finite difference grid points location.

Considering the aim of computations, relevant to the analysis of the transitional non-equilibrium of the flow phenomenon, it is assumed, for simplicity, that there is some local equilibrium between both phases in the inlet boundary section γ_1.

Thus the following boundary conditions are assumed in this section:

$$U_c(r) = U_d(r) = U_0(r), \quad \alpha_d(r) = \alpha_0, \quad k(r) = k_0(r),$$
$$\varepsilon(r) = \varepsilon_0(r), \quad V_c(r) = V_d(r) = 0.$$

The radial distributions of the velocity $U_0(r)$, the turbulence energy $k_0(r)$ and the dissipation rate $\varepsilon_0(r)$ were calculated in the same manner as for fully-developed turbulent pipe flow, on the basis of the method presented by DOBROWOLSKI and KABZA [23].

On the axis of the pipe symmetry γ_2, the boundary conditions are deduced from the assumed axial symmetry of the flowing stream:

$$V_c = V_d = \frac{\partial U_c}{\partial r} = \frac{\partial U_d}{\partial r} = \frac{\partial \alpha_d}{\partial r} = \frac{\partial k}{\partial r} = \frac{\partial \varepsilon}{\partial r} = 0.$$

At the outflow boundary γ_3 the boundary conditions for a greater part of the variables are prescribed arbitrarily:

$$V_c = V_d = \frac{\partial U_d}{\partial z} = \frac{\partial \alpha_d}{\partial z} = \frac{\partial k}{\partial z} = \frac{\partial \varepsilon}{\partial z} = 0.$$

For the axial component U_c of the velocity vector of the continuous phase, the following continuity condition is assumed:

$$\dot{M}_c|_{\gamma_3} = \dot{M}_c|_{\gamma_1},$$

where $\dot{M}_c$ denotes the mass flow ratio.

The effect of the boundary conditions prescribed arbitrarily in the section γ_3 on the flow field near the orifice may be reduced by a sufficiently long distance of the cross-section γ_3 from the orifice.

On the solid walls γ_4, the boundary conditions for the continuous phase equations are deduced from the applied version of the $k-\varepsilon$ turbulence model for the high Reynolds number flow as shown in the paper by LAUNDER and SPALDING [15] and RODI [22].

For the dispersed phase the following conditions are assumed:

$$\frac{\partial \alpha_d}{\partial n} = V_d = U_d = 0,$$

where n is the normal direction to the wall.

In a part of the computations, when the dispersed phase was treated as an inviscid one, a different form of these conditions was applied:

$$\frac{\partial \alpha_d}{\partial n} = \frac{\partial (\mathbf{U}_d)_t}{\partial n} = (\mathbf{U}_d)_n = 0,$$

where the subscripts t and n refer to tangential and normal-to-the wall components of the velocity vector for the dispersed phase, respectively.

3.3. Numerical procedure

The considered flow is difficult to solve, even in the case of a simple homogeneous fluid, when the flow phenomenon is described by the Navier–Stokes equations. This results from the sudden stream contraction in the section before the pipe orifice and recirculating flow behind the orifice. Both factors mentioned above are the reason of numerical difficulties connected, on the one hand, with the effect of the additional numerical diffusion, introduced by the upwind differencing schemes, applied for the sollution of elliptical flow problems, and on the other hand, with the necessity of applying fine grid spacing in the zone of stream contraction. The mentioned problems and methods of their solutions have been discussed at large by RAITHBY [24], SHYY and CORREA [25] and CASTRO [26]. To reduce the effect of the additional numerical diffusion the SUDS differencing scheme as proposed by RAITHBY [28] was applied in the paper by DOBROWOLSKI and KABZA [27]. In work by NIGRO *et al.* [29], in order to obtain more accurate calculations in the zone of stream contraction, a specially designed semi-orthogonal grid was used.

In some papers, e.g. by POPE [30] and SHYY *et al.* [31], special computational methods, relevant to the use of general orthogonal and non-orthogonal finite-difference grids, were proposed in order to achieve more accurate computations in the prediction of recirculating flow.

In two-phase flow it is necessary to solve the sets of equations for both phases, which makes new problems connected with the presence of interphase couplings. Appropriate

algorithms, characterized by a high degree of implicity, are presented in the papers by SPALDING [32] and LEE [33].

In the case of the flow considered in the present paper and on account of the assumed small volume fraction α_d of the dispersed phase, it is possible to apply a simplified calculation scheme.

The solution of the set of equations given in Sect. 3.1 is based on the extension of algorithms applied in the paper by DOBROWOLSKI and KABZA [23] for the calculation of a turbulent flow through a pipe orifice.

The computational area is discretized by the finite-difference grid as shown in Fig. 2. Computational cells and main grid points are given in Fig. 3.

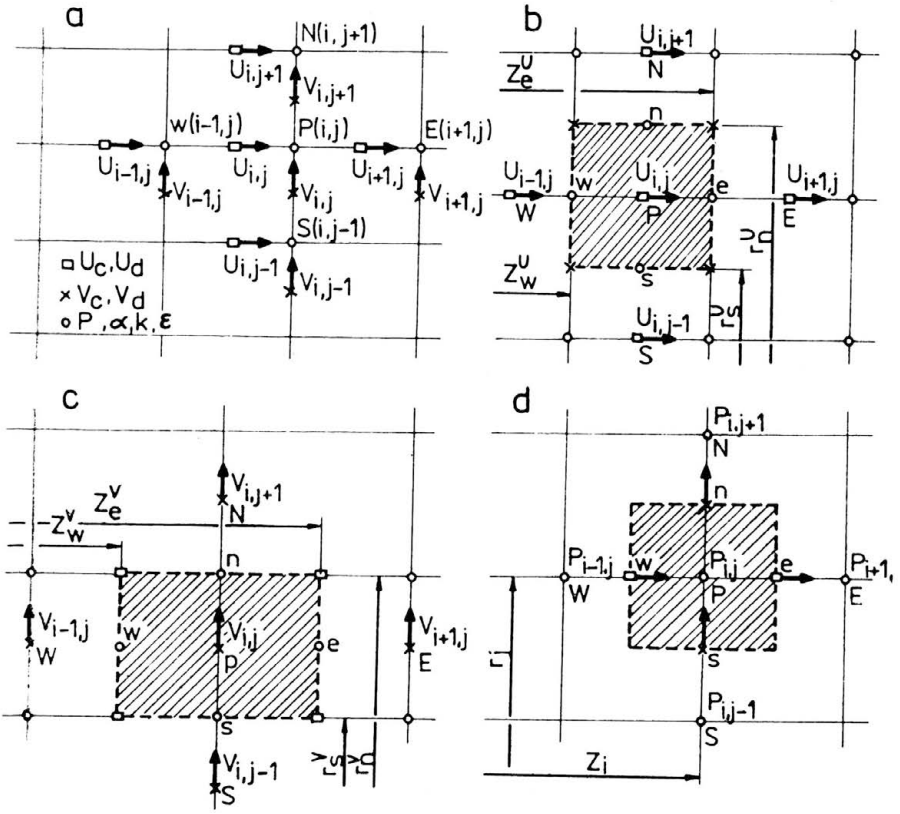

FIG. 3. The finite difference cells and notations; a) general finite-difference grid and variables location b) grid type U for axial velocity components, c) grid type V for radial velocity components, d) grid type P for pressure.

The axial components U_c and U_d and radial components V_c and V_d of the velocity vectors of both phases as well as the variables p, k, ε and α_d are defined in various grid points. Consequently this leads to making use of three displaced grid types U (Fig. 3b), V (Fig. 3c) and P (Fig. 3d).

On account of the similarity of form of the equations of motion and the turbulence model equations, these are discretized in a similar manner. In consequence, for each internal grid point, the following form of general algebraic equation was obtained:

$$(a_P^{\Phi}+S_{P,\Phi})\Phi_P = a_E^{\Phi}\Phi_E+a_W^{\Phi}\Phi_W+a_N^{\Phi}\Phi_N+a_S^{\Phi}\Phi_S+S_{U,\Phi}, \tag{3.12}$$

where Φ denotes a general dependent variable and the subscripts P, N, E, S and W concern points of difference grid Fig. 3b–3d, appropriate for a given variable. The components a^{Φ} in Eq. (3.12) are calculated on the basis of the finite-differential approximation of convective and diffusive terms of differential equations. The appropriate computational algorithms are given in the paper by GOSMAN and PUN [34], KOLNIAK *et al.* [35] and by PATANKAR [36]. The additional source terms refer to the use of the rest of the equation components not included in the coefficients a^{Φ}. Thus, for example, for Eq. (3.3) ($\Phi = U_c$) these components have the form

$$S_{P,U_c} = F_p VU, \tag{3.13}$$

$$S_{U,U_c} = DU(p_W-p_P)+\left(F_P(U_d)_P+S_{VIS}\right)VU, \tag{3.14}$$

where

$$VU = r_P^U(z_e^U-z_w^U)(r_n^U-r_s^U),$$

$$DU = (\alpha_c)_w\frac{r_n^U+r_s^U}{2}(r_n^U-r_s^U);$$

the notation used is given in Fig. 3b.

In order to improve the convergence, the component $F(U_d-U_c)$ is approximated in a semi-implicit manner.

The presence of new components in the standard form of transport equations for k and ε requires the modification of a computational scheme for homogeneous fluids.

The components $S_{P,k}$ and $S_{U,k}$ of Eq. (3.10) are calculated as follows

$$S_{P,k} = \left(\alpha_c^2\frac{c_\mu \varrho_c^2 k}{\mu_t}+F\right)VP, \tag{3.15}$$

$$S_{U,k} = \left(\alpha_c\mu_t G+Fk\int_1^{10,000}\frac{\Omega_1-\Omega_R}{\Omega_2}E(\omega)\,d\omega\right)VP, \tag{3.16}$$

where VP denotes the control volume of the grid type "P" shown in Fig. 3d. The integral term in Eq. (3.16) is calculated on the basis of the second order accuracy method and the interval of integration is divided into 150 nonuniform parts.

The presence of the integral term in the finite difference equations for the turbulence model increases the computer time considerably since the component must be calculated in every grid point at each iteration level.

The equation of continuity (3.2) was used for the evaluation of the pressure correction p' on the basis of the SIMPLE [36] method.

The distribution of the volume fraction α_d of the dispersed phase in the two-phase stream was computed from Eq. (3.1). The discretization of this equation on the grid type P (Fig. 3d) leads to the difference equation

$$A_{ew}^p(\alpha_d U_d)_e-A_{ew}^p(\alpha_d U_d)_w+A_{ns}^p(\alpha_d V_d)_n-A_{ns}^p(\alpha_d V_d)_s = 0. \tag{3.17}$$

The values of the expressions in brackets are calculated on the basis of the upwind differencing scheme, e.g. for the point e we obtain

$$(\alpha_d U_d)_e = \frac{1}{2}\{[\alpha_d]_E(U_e - |U_e|) + [\alpha_d]_P(U_e + |U_e|)\}. \tag{3.18}$$

After substitution of the equations of the type (3.18) for the points s, n and w of the difference grid to Eq. (3.17), the Poisson equation is obtained for the computation of the distribution α_d.

Considering the nonlinearity of the sets of difference equations and interphase couplings, it was necessary to apply some relaxation techniques.

Equation (3.12) may be written down in the modified form

$$\tilde{\Phi}_P^{n+1} = \frac{\sum\limits_{N,S,E,W} a_i^{\phi} \Phi_i^n + S_{U,\phi} + I\Phi^n}{\sum\limits_{N,S,E,W} a_i^{\phi} + S_{P,\phi} + I}, \tag{3.19}$$

where n means successive iteration number. In order to improve the stability, a fictitious source term $I(\Phi^{n+1} - \Phi^n)$ was introduced. Equation (3.19) shows that if I is very large, only a small change can occur in the value of Φ. This plays an important role in the initial phase of the iterative process. The relaxation parameter $I \geqslant 0$ was selected on the basis of the mass balance in each elementary cell of the difference grid.

On account of the fact that for the convergent solution

$$\lim_{n \to \infty} I(\Phi^{n+1} - \Phi^n) = 0,$$

the introduced relaxation parameter does not affect the solution.

The sets of difference equations (3.12) for particular variables were solved by the block "line by line" iteration method. In the internal iterative cycles the following under-relaxation was applied:

$$\Phi^{n+1} = \beta\tilde{\Phi}^{n+1} + (1-\beta)\Phi^n,$$

where β denotes the relaxation parameter.

The values of β were selected separately for each variable. The solution for a homogeneous fluid was assumed as an initial distribution for the two-phase flow.

The presented calculation scheme is characterized by good convergence for the low values of α_d (typical value of $\alpha_d = 0.005$ or less). In case of higher values of α_d, the conver gence becomes slow and it is then necessary to use a more complex algorithm, e.g. IPSA proposed by SPALDING [32].

3.4. Results of calculations

A series of numerical calculations for an orifice with the area ratio $m = (d/D)^2 = 0.4$, installed in a pipe of the diameter $D = 0.081$ m, has been carried out. In all the presented computational examples there is assumed the constant value of the Rynolds number $\mathrm{Re} = U_0 D\varrho_c/\mu_c = 9 \cdot 10^4$ where $U_0 = 18.6$ m/s is the mean gas velocity in the cross-section before the orifice. The density ratio $\varrho_d/\varrho_c = 1000$ is assumed. The uniform volume

fraction distribution $\alpha_d = 0.001$ corresponding to the loading ratio $Y = \dot{M}_d/\dot{M}_c = 1$ is assumed in the inlet section.

All the computations presented below were performed with a grid of 14 points in the r direction and 31 points in the z direction, because of the limited speed and storage of the used computer (ODRA 1305).

A comparison of turbulence models, the purpose of which is to estimate the influence of the microstructure of a two-phase stream upon the time-mean flow fields of both phases, is presented below. Three versions of a turbulence model are used: the first one excluding

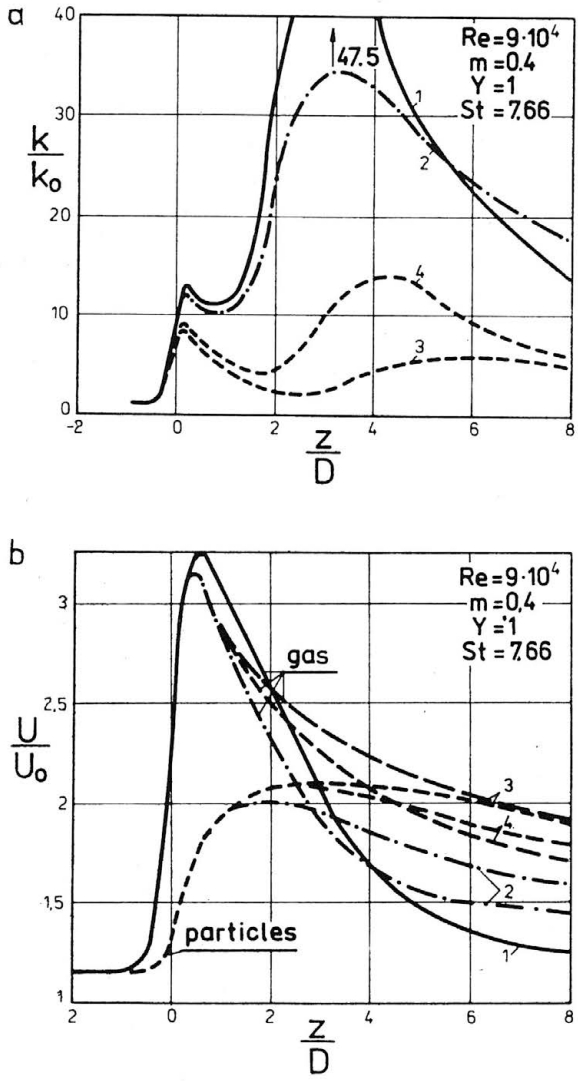

FIG. 4. a) Axial distributions of normalised turbulence energy. b) Axial distributions of both normalised phases axial velocity components; *1* — homogeneous flow, *2* — nonequilibrium flow with basic $k-\varepsilon$ model, *3* — nonequilibrium flow with maximum source terms in $k-\varepsilon$ model, *4* — nonequilibrium flow with proposed version of turbulence model.

the influence of particles (S_p^k, $S_p^\varepsilon = 0$), the second one including the maximum influence of particles on the turbulence kinetic energy ($S_p^k = 2Fk$, $S_p^\varepsilon = -2F\varepsilon$) and the third one based on the Chao solution ($S_p^k = -\alpha_c \varrho_c \varepsilon_a$, $S_p^\varepsilon = -\frac{\varepsilon}{k}\alpha_c \varrho_c \varepsilon_a$, where ε_a is calculated from Eq. (2.19).

The results of calculations for particles of the diameter $d_p = 100$ μm are presented in Figs. 4a and 4b, and they are compared with the appropriate solutions for homogeneous flow. In homogeneous fluid flow (curve 1) it is possible to observe a big increase in the initial turbulence intensity behind the orifice, brought about by the action of shear stresses ocurring on the boundary of the recirculating zone. The presence of particles in the stream suppresses the turbulence velocity fluctuations to a great extent.

In the case of the zero values of the additional source terms in the turbulence model equations (curve 2), only the influence of changes of time-mean variables upon the turbulence energy is included.

Whereas, in the case of the nonzero values of the S_p^k and S_p^ε terms, some considerably additional dissipation of the turbulence energy is noticed, especially in the expansion section of the flowing stream.

The attenuated influence of particles on the turbulence energy is also connected with the increase in the volume fraction of the dispersed phase in the symmetry axis behind the orifice.

The microstructure of the stream considerably influences the velocity distributions along the symmetry axis in the expansion section of the stream (Fig. 4b).

In order to analyse more widely the transitional nonequilibrium of flow and the interphase coupling effect, a series of numerical calculations were carried out for particles of the diameters $d_p = 10 \div 200$ μm.

With the values of the rest of the parameters considered in the calculations, the Stokes number

$$\text{St} = \varrho_d \frac{d_p^2 U_0}{18 \mu_c D} \tag{3.20}$$

is contained within the interval: St = 0.076–30.6.

While considering the weak dependence of the time-mean variables of both phases upon the turbulence in the section of a stream contraction, $S_p^k = S_p^\varepsilon = \mu_{dt} = 0$ is assumed

This allows to lessen the costs of computations connected with the analysis of the two-phase flow phenomenon in the immediate vicinity of the orifice. The radial distributions of the axial velocity vector components U_c and U_d of both phases in the selected cross-section of the flow system are presented in Fig. 5. These results correspond to the loading ratio $Y = 1$ and various values of the Stokes number. The great dependence of velocity distributions of the dispersed phase upon the value of the Stokes number can be noticed. With $St \to 0$ the velocity differences of both phases are small and they occur only near the orifice region. As the values of St rise, the degree of the non-equilibrium flow phenomenon increases and with value of St = 30.6 the dispersed phase undergoes only some slight acceleration. The axial distributions of the velocity of both phases along the duc t axis are presented in Fig. 6.

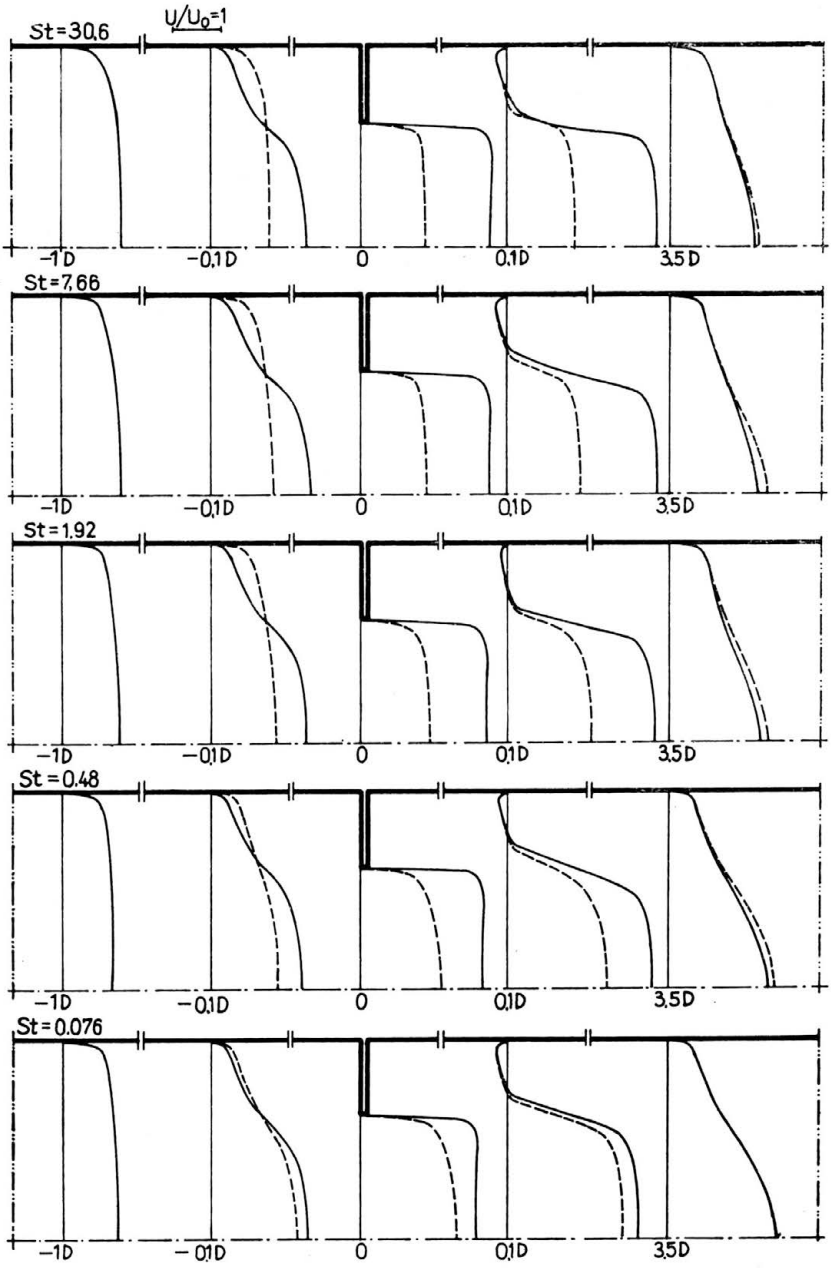

FIG. 5. The radial distributions of the axial velocity profiles.

The presented results point out the fact that the cross-sections "vena contracta", in which the maximum velocities of both phases occur, are displaced in relation to one another. Up to the present the factor has not been taken into consideration in the formulation of one-dimensional models.

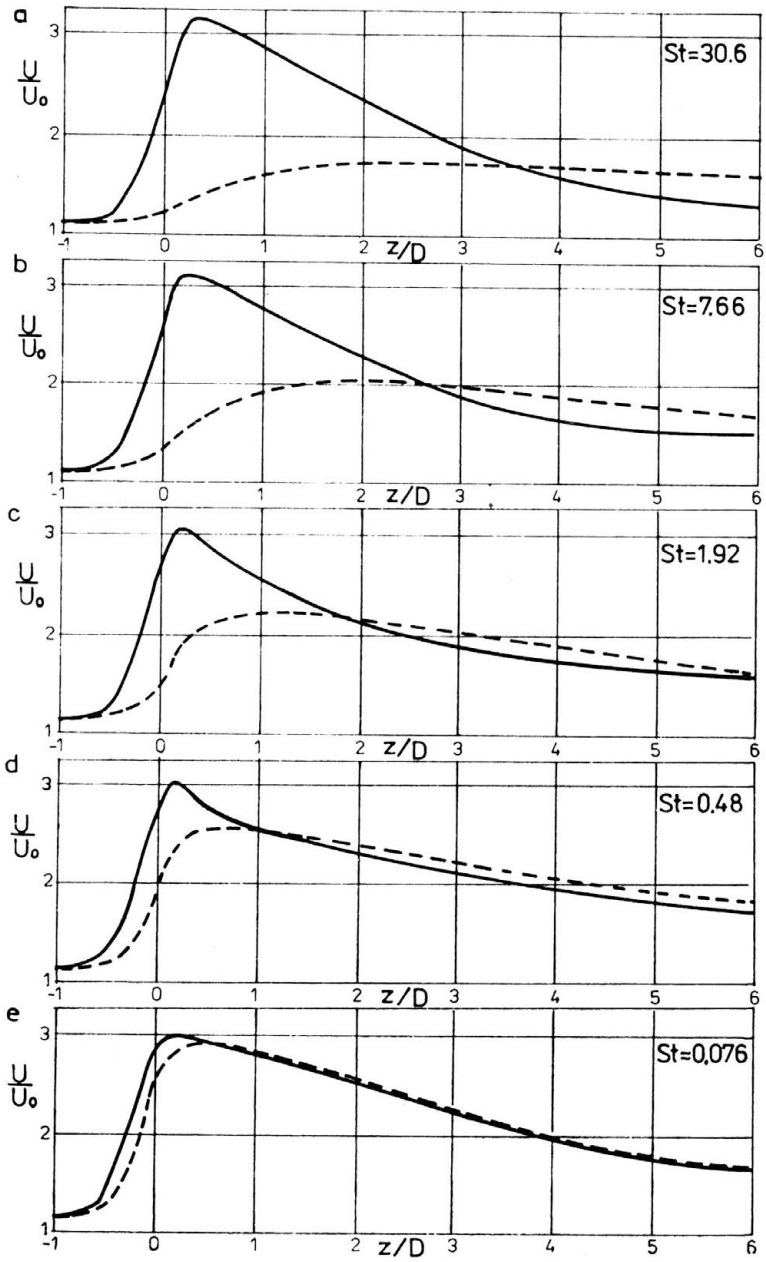

FIG. 6. The axial distributions of normalized axial velocity components of both phases. a) $d_p = 200$ μm, b) $d_p = 100$ μm, c) $d_p = 50$ μm, d) $d_p = 25$ μm, e) $d_p = 10$ μm.

The transitional nonequilibrium of the flow phenomenon causes the nonuniform distribution of the volume fraction α_d of the dispersed phase.

The radial distributions of the void fraction α_d of the dispersed phase are presented in Fig. 7. They point out the great dependence of the volume fraction distribution upon

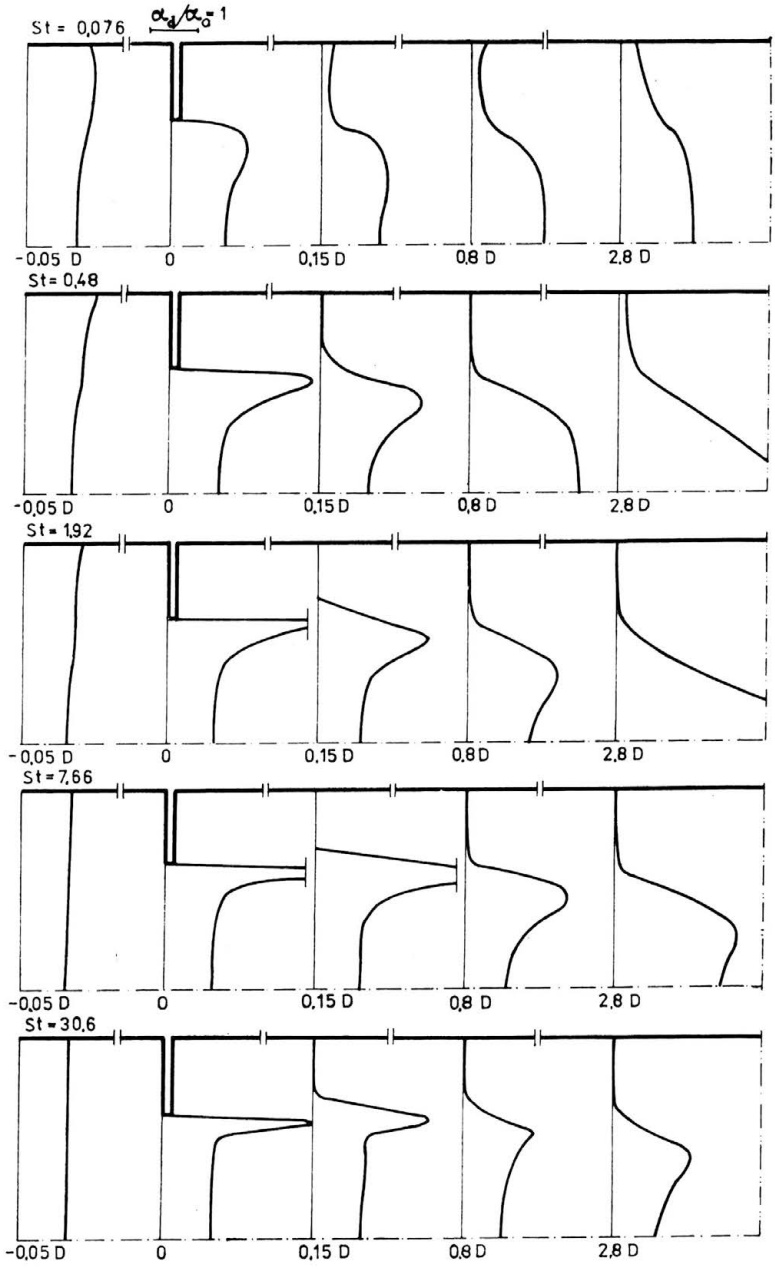

FIG. 7. The radial distributions of the void fraction α_d of the dispersed phase.

the value of the Stokes number. In the case of large particles a considerable increase in the local volume fraction near the axis of symmetry behind the orifice can be observed. To explain this effect, the particle trajectories were calculated by the method given in the paper by DOBROWOLSKI [37]. The paths of particles leaving the inlet section with the veloc-

ity equal to the local velocity of gas were calculated from the integration of the single particle motion equation in the velocity field of the gaseous phase. The results of calculations are presented in Fig. 8. They correspond to the assumption that particle collisions with the pipe orifice surface are of a perfectly elastic character.

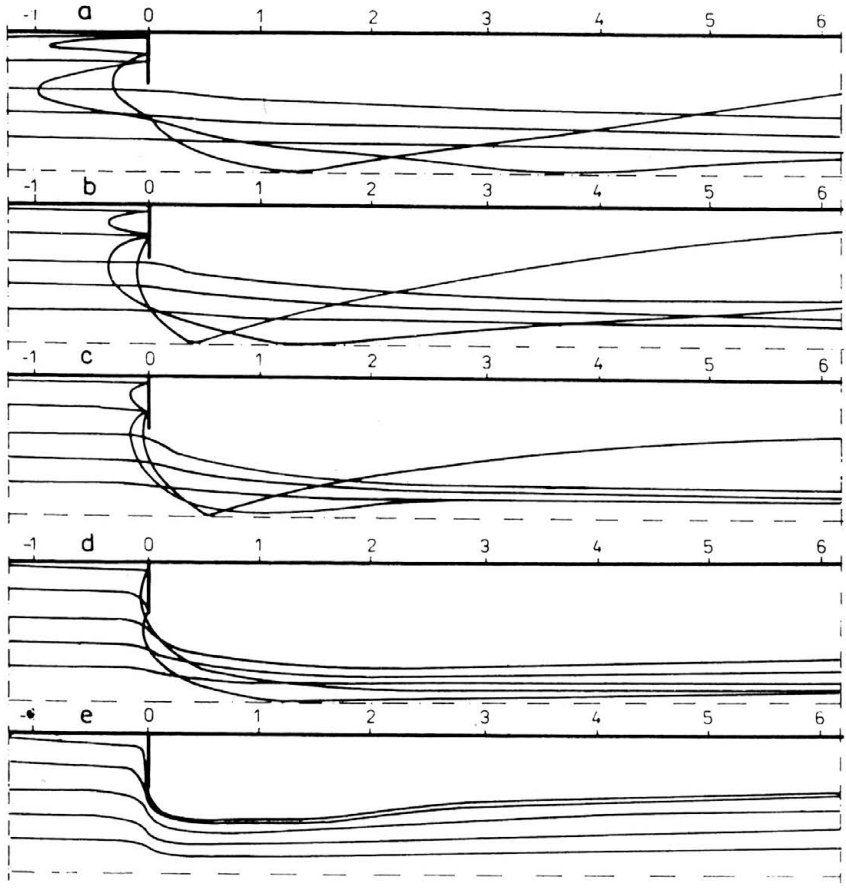

FIG. 8. The particles trajectories in the case of perfectly elastic collision with the surface of the pipe orifice; a) $d_p = 200$ μm, b) $d_p = 100$ μm, c) $d_p = 50$ μm, d) $d_p = 25$ μm, e) $d_p = 10$ μm.

The dependence of particle trajectories upon their diameters, closely connected with the non-equilibrium of flow, is noticed. The paths of particles of the diameter $d_p = 10$ μm are close to those of fluid elements. With the increase in the diameter d_p of particles, their trajectories differ considerably from the stream-lines of the continuous phase, and with $d_p = 200$ μm very complex trajectories are observed. Large particles glance off the orifice wall and cross the symmetry axis.

As a result of trajectory concentration near the axis of symmetry and the decrease in the velocity of the dispersive phase, as shown in Fig. 5, there occurs the local increase in the volume fraction in the area behind the pipe orifice.

The influence of the Stokes number upon the pressure distributions at the pipe wall for the constant loading ratio Y is presented in Fig. 9. Pressure distributions and, at the

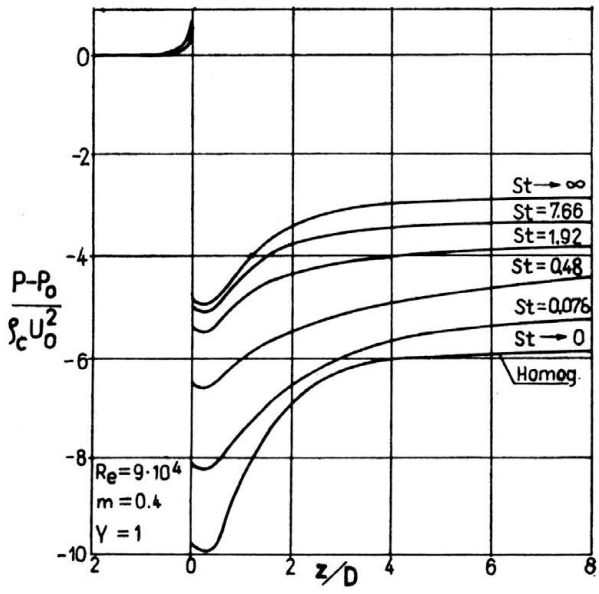

FIG. 9. The pressure distributions at the pipe wall as a function of the Stokes number.

same time, the differential pressure Δp are generally affected by the presence of particles and especially by the particle size diameter d_p.

The essential influence upon the increase in the differential pressure Δp_{tp} in a two-phase flow is exerted by the particles of small diameters. A similar conclusion was reached by DOBROWOLSKI *et al.* [38] for laminar flow through a pipe orifice and by DI GIACINTO *et al.* [39] for laminar flow through a duct with a sudden restriction. The dependence of the differential pressure on the loading ratio Y and the Stokes number is shown in Fig. 10. The differential pressure Δp_{tp} varies linearly with the loading ratio Y, thus it can be written down as

$$\frac{\Delta p_{tp}}{\Delta p_c} = 1 + f(\mathrm{St})\, Y, \tag{3.21}$$

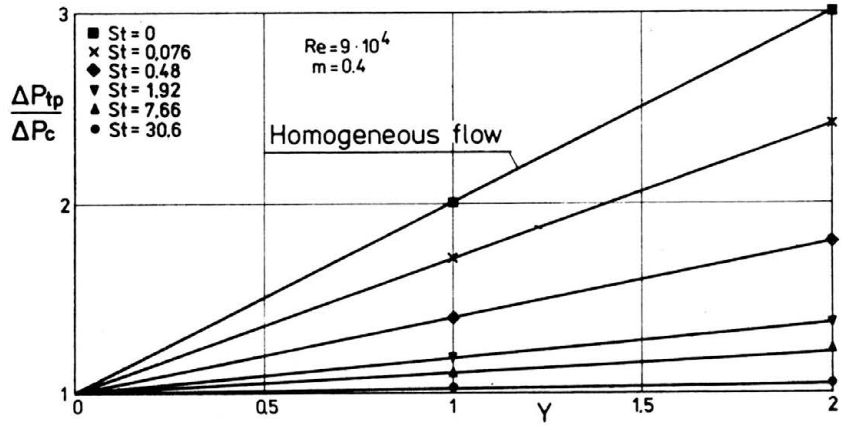

FIG. 10. The differential pressure Δp_{tp} as a function of loading ratio Y.

where Δp_c corresponds to the pressure drop of the continuous phase alone and the function $f(\mathrm{St})$ is strongly dependent on the Stokes number.

The linear dependence of the differential pressure Δp_{tp} as the function of the loading ratio is also found in the above-quoted papers by DOBROWOLSKI *et al.* [38], DI GIACINTO *et al.* [39] as well as by SHARMA and CROWE [40], LEE and CROWE [41] and DOSS [42], for a two-phase flow through a Venturi tube, but up to now no attempt has been made to establish any forms and arguments of the function f.

Since the differential pressure in a two-phase flow is contained within the interval $\Delta p_c \leqslant \Delta p_{tp} \leqslant \Delta p_H$, where the value of Δp_H corresponds to a homogeneous mixture flow and Δp_c is related to a pure gas flow, the function $f(\mathrm{St})$ has to satisfy the following asymptotic conditions:

$$\lim_{\mathrm{St}\to 0} f(\mathrm{St}) = 1, \qquad \lim_{\mathrm{St}\to\infty} f(\mathrm{St}) = 0.$$

On the grounds of a number of numerical calculations from laminar [38] and turbulent flows, the following form of the non-equilibrium correction $f(\mathrm{St})$ is proposed:

$$f(\mathrm{St}) = \left\{1+\exp\left[A\left(\ln\left(18\ \mathrm{St}\sqrt{m}\right)-B\right)\right]\right\}^{-1}, \tag{3.22}$$

where for the pipe orifice flow the constants A and B are equal to 0.9 and 1.2, respectively. The graph of the function $f(\mathrm{St})$ and numerical data are presented in Fig. 11.

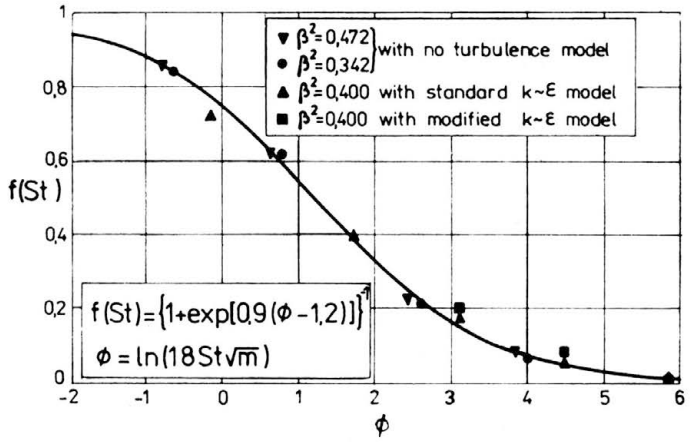

FIG. 11. The graph of the function $f(\mathrm{St})$.

The proposed function (3.22) approximates the numerical data and, moreover, it satisfies the asymptotic conditions.

The term St can be defined by

$$\mathrm{St} = \frac{1}{18}\frac{\varrho_d}{\varrho_c}\left(\frac{d_p}{D}\right)^2 \mathrm{Re}_c. \tag{3.23}$$

The definitions (3.23) differ from the Stokes number (3.20) only by introducing the non-dimensional similarity groups.

Thus, the proposed form of the function f conditions the pressure drop in a non-equilibrium two-phase flow on the values of four nondimensional similarity groups: the density ratio ϱ_d/ϱ_c, the scale ratio d_p/D, the Reynolds number for the continuous phase Re_c and

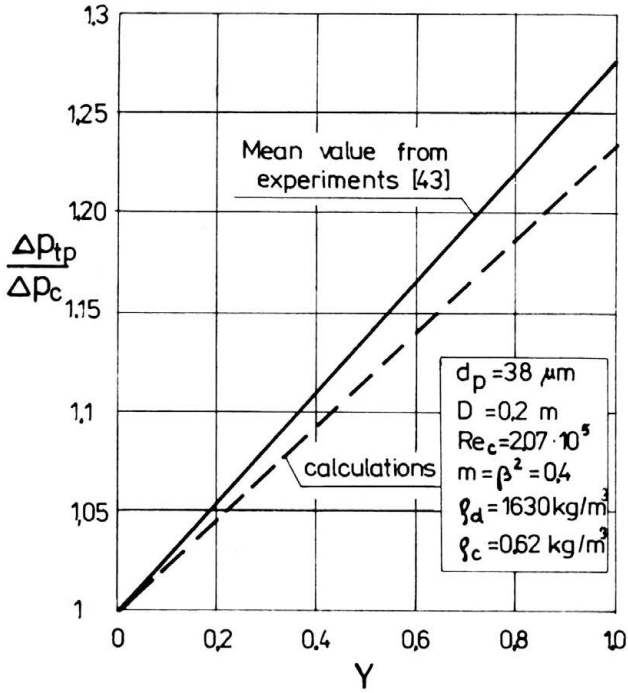

FIG. 12. Comparison between experimental data and the result of calculations.

the area ratio m. Figure 12 presents a comparison between the theoretical results based on Eqs. (3.21) and (3.22) and the experimental data of KESOVA *et al.* [43] for the pressure drop versus the loading ratio for an orifice with area ratio $m = 0.4$. The calculations were performed for the equivalent mean diameter $d_p = 38$ μm based on the discrete particle size distribution function. A good agreement exists between the predictions and the experiment.

As shown in the recent paper by DOBROWOLSKI and KABZA [44], the function $f(\mathrm{St})$, after some slight modification of the constants A and B, can be used for the prediction of the pressure drop in a Venturi tube and it allows to obtain good results of calculations with regard to the experimental data.

4. Conclusion

The presented computational model permits to include the non-equilibrium of the flow phenomenon and the influence of particles upon the microstructure of a turbulent two-phase stream. Some additional source terms in the transport equations for the kinetic turbulence energy and the dissipation rate have been introduced in a theoretical manner and the evaluations carried out point out their correct asymptotic behaviour. The conducted numerical investigations of transitional non-equilibrium recirculating flow, based on the proposed computational scheme show that the additional source terms S_p^k and S_p^ε may be neglected in the stream-contraction problems but they have to be included into the considerations in the case of stream-expansion problems.

As a result of the numerical study, the interphase coupling effects of the velocity, volume, fraction and pressure fields have been analysed. It has been found that the basic parameters for turbulent dilute suspension flow are the Stokes number and the loading ratio.

A simple form of the non-equilibrium correction function, based on four nondimensional similarity groups, has been proposed for the calculation of the pressure drop in the case of transitionally non-equilibrium dispersed two-phase flow.

References

1. F. H. Harlow, A. A. Amsden, *Numerical calculation of multiphase fluid flow*, J. Comp. Physics, **17**, 19–52, 1975.
2. C. W. Rivard, M. D. Torrey, K-FIX: *A computer program for transient, two-dimensional, two-fluid flow*, LASL Report LA-NUREG-6623, April 1977.
3. D. B. Spalding, *Numerical computation of multiphase flow*, Lecture Series 1981–82, von Kármán Institute for Fluid Dynamics, Belgium.
4. D. Migdal, V. D. Agosta, *A source flow model for continuous gas particle flow*, Trans. ASME, J. Appl. Mech., **35**, 860–867, 1967.
5. C. T. Crowe, M. P. Sharma, D. E. Stock, *The particle source-in-cell method for gas-droplet flow*, Trans. ASME, J. Fluid Engng., **99**, 325–332, 1977.
6. J. K. Dudkiewicz, *A particle fluid numerical model for liquid sprays*, J. Comp. Physics, **35**, 229–253, 1980.
7. M. Maeda, K. Hishida, *Velocity and turbulence intensity measurement of gas and spherical particles in two-phase flow by modified LDA-system*, Sensor '82, 12–14 Jan., 1982, Essen.
8. Y. Tsuji, Y. Morikawa, H. Shiomi, *LDV measurements of an air-solid two-phase flow in a vertical pipe*, J. Fluid Mech., **139**, 417–434, 1984.
9. D. Modarress, J. Wuerer, S. Elgobashi, *An experimental study of a turbulent round two-phase jet*, AIAA/ASME 3rd Joint Termophysics, Fluids, Plasma and Heat Transfer Conference, June 7–11, 1982, St. Louis.
10. A. D. Gosman, E. Ioannides, *Aspects of computer simulation of liquid-fuelled combustors*, AIAA Paper 81–0323, 19th, Aerospace Science Meeting, St. Louis, 1981.
11. H. Danon, M. Wolfshtein, C. Hetsroni, *Numerical calculations of two-phase turbulent round jet*, Int. J. Multiphase Flow, **3**, 223–234, 1977.
12. S. E. Elgobashi, T. W. Abou-Arab, *A two-equation turbulence model for two-phase flows*, Phys. Fluids, **26**, 931–938, 1983.
13. S. Elgobashi, T. Abou-Arab, T. Rizk, A. Mostafa, *Prediction of the particle-laden jet with a two-equation turbulence model*, Int. J. Multiphase Flow, **10**, 697–710, 1984.
14. A. A. Mostafa, S. F. Elgobashi, *A two-equation turbulence model for jet flows laden with vaporizing droplets*, Int. J. Multiphase Flow, **11**, 515–535, 1985.
15. B. E. Launder, D. B. Spalding, *The numerical computation of turbulent flows*, Comp. Meth. Appl. Mech. Engng., 3, 269–289, 1974.
16. S. L. Soo, *Fluid dynamics of multiphase system*, Blaisdell Publ. Co., Waltham 1967.
17. F. Dobran, *Constitutive equations for multiphase mixtures of fluids*, Int. J. Multiphase Flow, 10, 272–305, 1984.
18. D. A. Drew, R. T. Lahey, *Application of general constitutive principles to the derivation of multi-dimensional two-phase equations*, Int. J. Multiphase Flow, **5**, 243, 246, 1979.
19. R. I. Peskin, *Stochastic estimation applications to turbulent diffusion*, Int. Symp. Stochastic Diffusion, University of Pittsburgh, 1971.
20. Zh. D. Genchev, D. S. Karpuzov, *Effects of the motion of dust particles on turbulence transport equation*, J. Fluid Mech., 101, 833–842, 1980.

21. B. T. CHAO, *Turbulent transport behaviour of small particles in dilute suspension*, Österr., Ing., Arch., **18**, 7–21, 1964.
22. W. RODI, *Examples of turbulence-model applications*, Proc. of Ecole d'Ete d'Analyse Numerique, Clamart, 1982.
23. B. DOBROWOLSKI, Z. KABZA, *Application of mathematical modelling and digital simulation to the analysis of flow through the differential pressure type flowmeters* [in Polish], Postępy Technologii Maszyn i Urządzeń, 2, 69–82, 1983.
24. G. D. RAITHBY, *A critical evaluation of upstream differencing applied to problems involving fluid flow*, Comp. Meth. Appl. Mech. Engng, **9**, 75–103, 1976.
25. W. SHYY, S. M. CORREA, *A systematic comparison of several numerical schemes for complex flow calculations*, AIAA 23rd Aerospace Science Meeting, 14–17 Jan., Remo, 1985.
26. I. P. CASTRO, *Numerical difficulties in the calculation of complex turbulent flows*, Symposium on Turbulent Shear Flows, Pensylwania 1977.
27. B. DOBROWOLSKI, Z. KABZA, *Numerical analysis of laminar viscous flow through a pipe orifice*, Studia Geotechnica et Mechanica, **4**, 1–2, 29–46, 1982.
28. G. D. RAITHBY, *Skew upstream differencing schemes for problems involving fluid flow*, Comp. Meth. Appl. Mech. Engng., **9**, 75–103, 1976.
29. F. E. B. NIGRO, A. B. STRONG, S. A. ALPAY, *A numerical study of the laminar viscous incompressible flow through a pipe orifice*, ASME Paper 78-WA/FF-5.
30. S. B. POPE, *The calculating of turbulent recirculating flows in general orthogonal coordinates*, J. Comp. Physics, **26**, 197–217, 1978.
31. W. SHYY, S. S. TONG, S. M. CORREA, *Numerical recirculating flow calculations using a body-fitted coordinate system*, General Electric Report 84CRD027, 1984
32. D. B. SPALDING, *Numerical computation of multi-phase fluid flow and heat transfer*, in: Recent Advances in Numerical Mechanics, Ed. C. TAYLOR, Pineridge Press, 1980.
33. W. H. LEE, *A pressure iteration scheme for two-phase flow modelling*, LASL Report LA-UR-79-975, 1979.
34. A. D. GOSMAN, W. M. PUN, *Calculation of recirculative flows*, Lecture Notes, Imperial College of Science and Technology, London 1973.
35. P. KOLNIAK, A. PRZEKWAS, A. WANIK, *Method of modelling of recirculating flows* [in Polish], Wrocław Technical University Reports, No 25; Monograph Series No 8, Wrocław 1983.
36. S. PATANKAR, *Numerical heat transfer and fluid flow*, Hemisphere Publ. Corp., New York 1980.
37. B. DOBROWOLSKI, *Mathematical model of non-equilibrium turbulent flow of a two-phase polydispersive mixture* [in Polish], Symp. "Modelling in Mechanics "Kudowa (Poland), March 1986.
38. B. DOBROWOLSKI, Z. KABZA, A. SPYRA, *Numerical investigations of gas-solid mixture flow through a construction flow-meter*, JUREMA Proc., **29**, 73–76, 1984.
39. M. DI GIACINTO, F. SABETTA, R. PIVA, *Two-way coupling effect in dilute gas-particle flows*, Trans. ASME, J. Fluids Engng, 104, 304–311, 1982.
40. M. P. SHARMA, C. T. CROWE, *A novel physico-computational model for quasi-one-dimensional gas-particle flow*, Trans. ASME, J. Fluids Engng., **100**, 343–349, 1978.
41. J. LEE, C. T. CROWE, *Scaling laws for metering the flow of gas-particle suspension through Venturis*, Trans. ASME, J. Fluids Engng., **104**, 88–91, 1982.
42. E. D. DOSS, *Analysis and application of gas-solid flow inside a Venturi with particle interaction*, Int. J. Multiphase Flow, **11**, 445–458, 1985,
43. Л. А. КЕСОВА, В. Н. ЩЕВЧЕНКО, Х. Н. ЧЕРЕЗОВ, Ю. М. БУЛАВИЦКИИ, Б. А. ЧЕПУРНОИ, Р. М. ТАБАЧХИК, *Исследование пылерасходомеров с сужающими устройствами*, Теплоенепгетика, 3, 51-55, 1984
44. B. DOBROWOLSKI, Z. KABZA, *The theoretical evaluation of metrological performance of Venturi-meter under dispersed two-phase flow conditions*, JUREMA Proc., **31**, 43–46, 1986.

TECHNICAL UNIVERSITY OF OPOLE, OPOLE.

Received January 2, 1986.